Supporting Information: Charge scaling in classical force fields for lithium ions in polymers

Dongyue Liang, Yuxi Chen, Chuting Deng, and Juan J. de Pablo*

Pritzker School of Molecular Engineering, University of Chicago, Chicago, Illinois 60637, United States

E-mail: depablo@uchicago.edu

1 Simulation details

In this work, we apply a modified adaptive force matching technique[1] for parametrization. The system we use for parametrization contain 6 PEO_9 oligomers with -CH_3 and -O-CH_3 terminations (Fig. 1). For the two Li^+:EO ratios explored, which are 1:10 and 1:20, 6 or 3 Li^+-$TFSI^-$ ion pairs are added to the systems, respectively. This result in 528 or 480 atoms in total, and the equilibrated box dimensions are $\sim 17\times17\times17$ Å^3. As discussed in the main text, 5 systems are generated for each ratio.

The classical molecular dynamics (MD) simulations and density functional theory (DFT) calculations in the parametrization are performed with CP2K package.[2] The MD simulations are performed with the FIST module. The OPLS force field is used for PEO oligomers and ions.[3–5] The force field parameters adapted from OPLS force field are listed in Table S4, S5, S6 and S7. Smooth particle mesh Ewald[6,7] is used to treat the long-range electrostatic interactions, and a short-range non-bonded cutoff of 12 Å is applied. The MD simulations are performed with NPT ensemble. Nose-Hoover thermostat is applied for temperature control with a time constant of 10 fs. The barostat is applied with a pressure of 1 bar and a time constant of 1000 fs. During the parametrization, an annealing run of 1 ns at 500K is performed between the iterations. For each iteration, a production run of 1 ns is performed at respected temperatures, which are 300K or 373K. For the case of 1:10/20, 20/40 frames are extracted from the last 800 ps of each production trajectories for first-principles calculations.

The first-principles calculations are performed with the Quickstep module of CP2K.[2] The PBE functional[8] with Grimme's D3 empirical dispersion correction[9] is used. A cutoff of 600 Ry and relative cutoff of 60 Ry are applied. The Goedecker-Teter-Hutter (GTH) pseudopotentials are applied with the DZVP-MOLOPT-GTH basis sets. The calculations are performed at Gamma point level. Aside from the first-principle calculations performed for force matching, a Bader charge analysis was carried out with the Li^+:EO = 1:10 system with 528 atoms, as discussed in the main text. The code from Henkelman group[10–12] was used for the analysis.

The optimization required by force matching is performed by scripts written in Python. We applied Simplex algorithm, specifically Nelder-mead method[13] from the Scipy distribution[14] for the minimization. The objective function of each force matching optimization is written as:

$$Obj.\ Func. = \frac{\sum_{f=1}^{N_f} \sum_{i=1}^{N_{Li^+}} |\mathbf{F_{i,f,FF}} - \mathbf{F_{i,f,DFT}}|^2}{\sum_{f=1}^{N_f} \sum_{i=1}^{N_{Li^+}} |\mathbf{F_{i,f,DFT}}|^2} \quad (1)$$

Here N_f is the total number of frames used in the optimization. N_{Li} is the total number of Li^+ in each frame. $\mathbf{F_{i,f,FF}}$ and $\mathbf{F_{i,f,DFT}}$ are forces from force field and DFT calculations. The denominator of the objective function is a constant throughout the optimization, and can be omitted in practice.

For benchmarking, we performed large-scale MD simulations at multiple temperatures with OpenMM.[15] Each simulation box is assembled with 100 PEO_{35} chains with -CH_3 and -O-CH_3 terminations, and Li^+-$TFSI^-$ pairs corresponding to the Li^+:EO ratios, adding to $\sim$ 30000 atoms in total. The structures and input files are initially taken from the polymer builder module of CHARMM-GUI,[16–19] with modifications applied later with CHARMM[17] or manually. NPT ensemble is applied with 1 fs timestep. Particle mech Ewald[6,7] is applied to treat the electrostatics, and a cutoff of 12 Å is used for short-range interactions. Nose-Hoover thermostat is applied with a time constant of 1 ps. Monte Carlo barostat is applied with reference pressure of 1 bar and frequency of 100 steps. The simulations at temperatures of 450K or higher are run for 500 ns, where the first 10 ns is not used for diffusion analysis. The simulations at 300K and 333K are run for 100 ns. The interaction energy (Table S9) calculations were performed on the obtained trajectories with LAMMPS package.[20] The set-up of energy calculations are generally consistent with the MD simulations, except that Particle mesh Ewald is not applied for electrostatics. To compensate for that, the cutoff of electrostatic interactions is extended to 24 Å. VMD package is used for displaying the conformations.[21]

2 Supplemental tables and figures

Table S1: Optimization of parameters at Li^+:EO ratio of 1:20 and temperature of 300K. The objective function is defined as the mean-squared difference between force field forces and reference over the mean-squared forces. The units of ϵ and σ shown here are kcal/mol and Å.

Iteration	1	2	3	4	5	6	7
Scaling factor	1.0	0.80	0.81	0.80	0.80	0.80	0.80
$\epsilon_{Li-O(PEO)}$	0.05	0.06	0.06	0.06	0.06	0.06	0.06
$\sigma_{Li-O(PEO)}$	2.48	2.41	2.41	2.40	2.40	2.40	2.40
$\epsilon_{Li-O(TFSI^-)}$	0.06	0.06	0.06	0.06	0.06	0.06	0.06
$\sigma_{Li-O(TFSI^-)}$	2.51	2.36	2.35	2.34	2.34	2.34	2.34
Obj. Func.	33.0%	12.3%	10.3%	11.8%	11.0%	11.0%	11.3%

Table S2: Optimization of parameters at Li^+:EO ratio of 1:10 and temperature of 373K. The objective function is defined as the mean-squared difference between force field forces and reference over the mean-squared forces. The units of ϵ and σ shown here are kcal/mol and Å.

Iteration	1	2	3	4	5	6	7
Scaling factor	1.0	0.77	0.81	0.77	0.79	0.78	0.79
$\epsilon_{Li-O(PEO)}$	0.05	0.05	0.05	0.05	0.05	0.06	0.06
$\sigma_{Li-O(PEO)}$	2.48	2.42	2.42	2.40	2.41	2.40	2.40
$\epsilon_{Li-O(TFSI^-)}$	0.06	0.08	0.07	0.08	0.08	0.08	0.08
$\sigma_{Li-O(TFSI^-)}$	2.51	2.31	2.31	2.28	2.28	2.29	2.29
Obj. Func.	32.0%	11.3%	12.0%	10.3%	11.7%	11.0%	10.9%

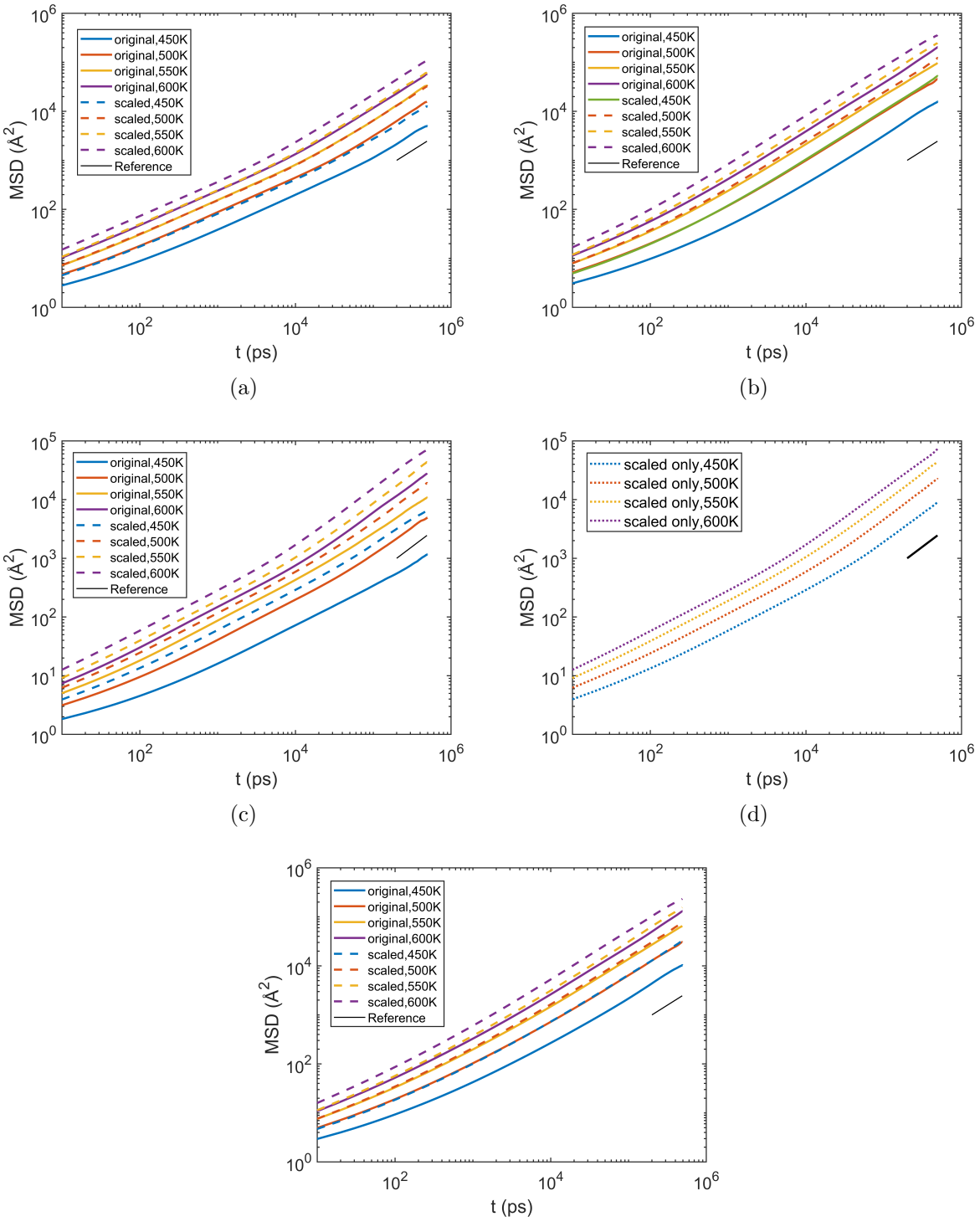

Figure S1: Mean-squared displacements for calculations of diffusion coefficients of ions. The figures (a-e) correspond to Li^+ for Li^+:EO=1:18, $TFSI^-$ for 1:18, Li^+ for 1:10, Li^+ for 1:10 with only the charge scaling factor applied (no LJ parameters modified from the original OPLS force field), and all ions for 1:18. The results suggest simulations at the length of several hundreds of nanoseconds are needed even at temperatures of 450K or higher.

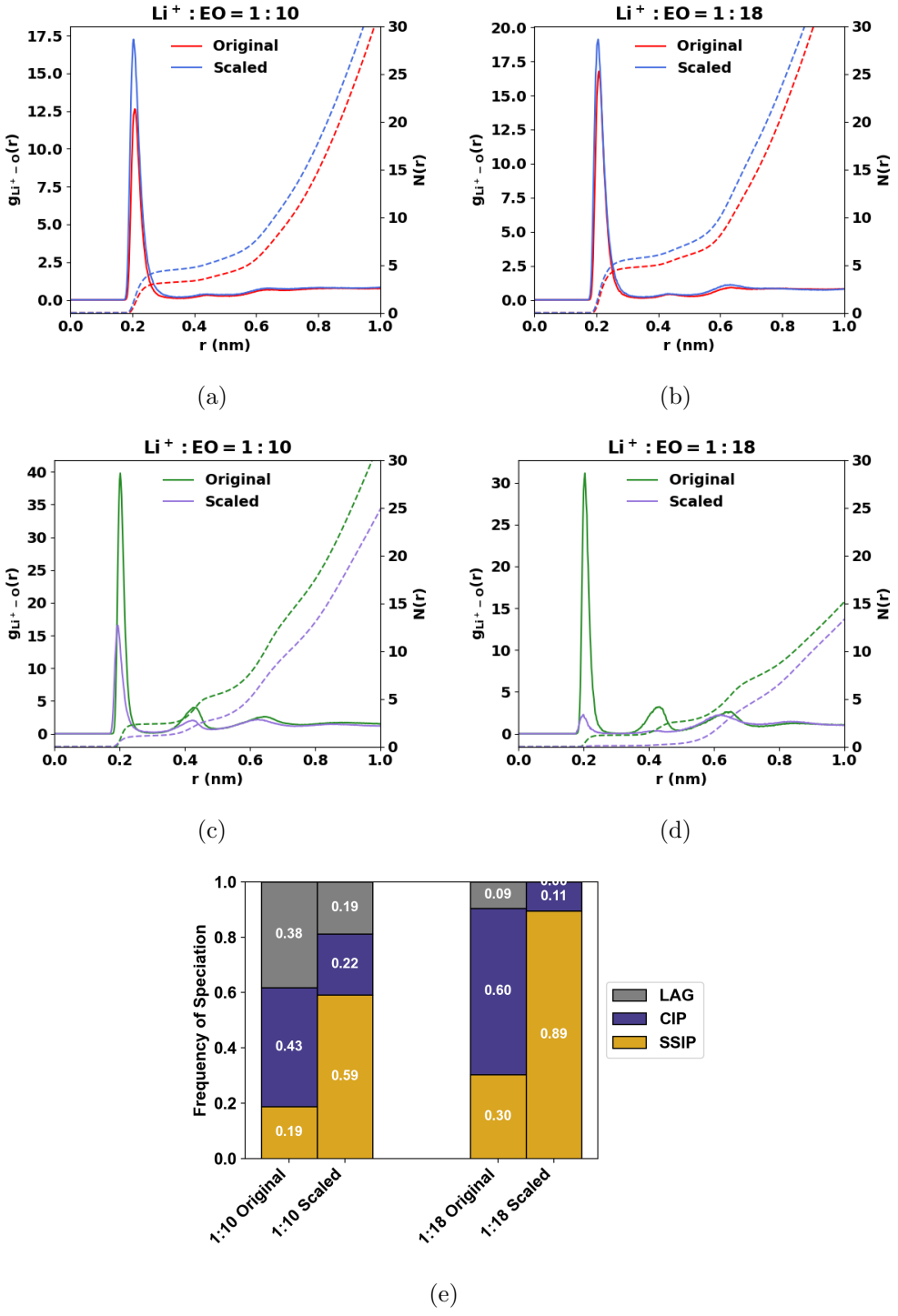

Figure S2: Radial distribution functions (a-d) and the frequency speciation of three most common conformational states (e) from MD simulations at 300K. Figures (a-d) show the RDF between Li^+ and PEO oxygens (a, b) and TFSI oxygens (c, d) at Li^+:EO ratios of 1:10 (a, c) and 1:18 (b, d). The result at 333K are shown in Fig. 3 and 4.

Table S3: Optimization of parameters at Li^+:EO ratio of 1:20 and temperature of 373K. The objective function is defined as the mean-squared difference between force field forces and reference over the mean-squared forces. The units of ϵ and σ shown here are kcal/mol and Å.

Iteration	1	2	3	4	5	6	7
Scaling factor	1.0	0.80	0.82	0.81	0.81	0.82	0.82
$\epsilon_{Li-O(PEO)}$	0.05	0.07	0.07	0.07	0.07	0.07	0.07
$\sigma_{Li-O(PEO)}$	2.48	2.36	2.36	2.36	2.36	2.36	2.36
$\epsilon_{Li-O(TFSI^-)}$	0.06	0.05	0.05	0.06	0.06	0.06	0.06
$\sigma_{Li-O(TFSI^-)}$	2.51	2.37	2.34	2.36	2.36	2.36	2.36
Obj. Func.	36.3%	13.6%	10.6%	11.9%	11.1%	11.1%	10.7%

Table S4: Non-bonded parameters used in this work from OPLS force field.[3–5] The units of charge, ϵ and σ shown here are e, kcal/mol and Å. The charges of Li^+ and $TFSI^-$ shown here are the values before charge scaling.

Atom type	charge	ϵ	σ
H (PEO)	0.03	0.03	2.5
C (PEO, CH_2)	0.14	0.066	3.5
C (PEO, CH_3)	0.11	0.066	3.5
O (PEO)	-0.4	0.14	2.9
Li	1.0	0.018	2.13
C (TFSI)	0.35	0.066	3.5
N (TFSI)	-0.66	0.17	3.25
O (TFSI)	-0.53	0.21	2.96
F (TFSI)	-0.16	0.053	2.95
S (TFSI)	1.02	0.25	3.55

Table S5: Bond parameters used in this work from OPLS force field.[3,4] The units are kcal/(mol·Å^2) for bond coefficients k and Å for bond length r.

Bond type	k	r
C-C (PEO)	268.0	1.529
C-O (PEO)	320.0	1.41
C-H (PEO)	340.0	1.09
C-F (TFSI)	441.92	1.323
N-S (TFSI)	374.88	1.57
C-S (TFSI)	233.03	1.818
S-O (TFSI)	637.07	1.437

Table S6: Angle parameters used in this work from OPLS force field.[3,4] The units are kcal/mol for angle coefficients K and degrees for equilibrium values θ.

Angle type	K	θ
C-C-H (PEO)	37.5	110.7
C-O-C (PEO)	60.0	109.5
H-C-H (PEO)	33.0	107.8
O-C-C (PEO)	50.0	109.5
O-C-H (PEO)	35.0	109.5
C-S-O (TFSI)	103.97	102.6
F-C-F (TFSI)	93.33	107.1
N-S-C (TFSI)	91.30	103.5
N-S-O (TFSI)	94.29	113.60
O-S-O (TFSI)	115.8	118.5
S-C-F (TFSI)	82.93	111.7
S-N-S (TFSI)	80.19	125.6

Table S7: Dihedral parameters used in this work from OPLS force field.[3,4] The units are kcal/mol.

Dihedral type	K_1	K_2	K_3	K_4
C-C-O-C (PEO)	0.65	-0.25	0.67	0
H-C-C-H (PEO)	0	0	0.3	0
H-C-C-O (PEO)	0	0	0.468	0
H-C-O-C (PEO)	0	0	0.76	0
O-C-C-O (PEO)	-0.55	0	0	0
N-S-C-F (TFSI)	0	0	0.316	0
O-S-C-F (TFSI)	0	0	0.347	0
S-N-S-C (TFSI)	7.833	-2.490	-0.764	0
S-N-S-O (TFSI)	0	0	-0.04	0

Table S8: Convergence test and error estimation data of the diffusion coefficient calculations of the ions. The temperatures (T) are listed in Kelvin. The diffusion coefficients (D) are listed in cm/s^2. The "original", "scaled" and "scaled-only" parameter sets correspond to the original OPLS force field parameters, charge-scaled force field with the modified LJ parameters, and without the modified LJ parameters presented in this work.

Li^+:EO	ion	T	parameter set	log-log slope	D(150ns)	D(250ns)	Error
1:18	Li^+	450	original	0.98	1.82×10^{-7}	1.80×10^{-7}	1.01%
1:18	Li^+	500	original	1.05	5.21×10^{-7}	5.35×10^{-7}	2.65%
1:18	Li^+	550	original	1.01	1.09×10^{-6}	1.10×10^{-6}	1.19%
1:18	Li^+	600	original	1.00	1.93×10^{-6}	1.93×10^{-6}	0.04%
1:18	Li^+	450	scaled	1.00	4.39×10^{-7}	4.41×10^{-7}	0.50%
1:18	Li^+	500	scaled	1.01	1.08×10^{-6}	1.08×10^{-6}	0.12%
1:18	Li^+	550	scaled	1.02	2.12×10^{-6}	2.14×10^{-6}	0.92%
1:18	Li^+	600	scaled	1.02	3.69×10^{-6}	3.73×10^{-6}	1.04%
1:18	$TFSI^-$	450	original	1.08	5.40×10^{-7}	5.60×10^{-7}	3.50%
1:18	$TFSI^-$	500	original	1.01	1.60×10^{-6}	1.59×10^{-6}	0.25%
1:18	$TFSI^-$	550	original	0.98	3.43×10^{-6}	3.39×10^{-6}	1.21%
1:18	$TFSI^-$	600	original	1.08	6.29×10^{-6}	6.54×10^{-6}	3.78%
1:18	$TFSI^-$	450	scaled	0.98	1.72×10^{-6}	1.71×10^{-6}	0.99%
1:18	$TFSI^-$	500	scaled	0.99	4.01×10^{-6}	3.97×10^{-6}	1.03%
1:18	$TFSI^-$	550	scaled	1.04	8.37×10^{-6}	8.56×10^{-6}	2.15%
1:18	$TFSI^-$	600	scaled	1.02	1.34×10^{-5}	1.34×10^{-5}	0.19%
1:18	all	450	original	1.05	3.61×10^{-7}	3.70×10^{-7}	2.40%
1:18	all	500	original	1.02	1.06×10^{-6}	1.06×10^{-6}	0.48%
1:18	all	550	original	0.99	2.26×10^{-6}	2.24×10^{-6}	0.62%
1:18	all	600	original	1.06	4.11×10^{-6}	4.24×10^{-6}	2.93%
1:18	all	450	scaled	0.99	1.08×10^{-6}	1.07×10^{-6}	0.68%
1:18	all	500	scaled	0.99	2.55×10^{-6}	2.53×10^{-6}	0.79%
1:18	all	550	scaled	1.04	5.25×10^{-6}	5.35×10^{-6}	1.91%
1:18	all	600	scaled	1.02	8.55×10^{-6}	8.58×10^{-6}	0.37%
1:10	Li^+	450	original	0.70	5.05×10^{-8}	4.33×10^{-8}	16.82%
1:10	Li^+	500	original	0.93	1.84×10^{-7}	1.78×10^{-7}	3.37%
1:10	Li^+	550	original	0.92	4.21×10^{-7}	4.05×10^{-7}	3.82%
1:10	Li^+	600	original	0.92	9.89×10^{-7}	9.52×10^{-7}	3.93%
1:10	Li^+	450	scaled	0.88	2.73×10^{-7}	2.57×10^{-7}	6.51%
1:10	Li^+	500	scaled	1.03	6.67×10^{-7}	6.71×10^{-7}	0.66%
1:10	Li^+	550	scaled	0.99	1.44×10^{-6}	1.43×10^{-6}	0.63%
1:10	Li^+	600	scaled	1.00	2.60×10^{-6}	2.60×10^{-6}	0.03%
1:10	Li^+	450	scaled-only	0.97	3.12×10^{-7}	3.07×10^{-7}	1.57%
1:10	Li^+	500	scaled-only	1.03	7.59×10^{-7}	7.67×10^{-7}	1.07%
1:10	Li^+	550	scaled-only	1.00	1.48×10^{-6}	1.48×10^{-6}	0.02%
1:10	Li^+	600	scaled-only	0.97	2.49×10^{-6}	2.44×10^{-6}	2.09%

Table S9: Averaged interaction energies between a Li^+ and rest of the system from MD simulations at 300K, with the decomposition to electrostatic and van der Waals interactions. The unit of the energies is kcal/mol.

Li^+:EO	parameter set	$\langle \bar{E} \rangle$	$\langle \bar{E}_{elec} \rangle$	$\langle \bar{E}_{vdW} \rangle$
1:18	original	-206.2 ± 23.2	-212.3 ± 23.1	6.0 ± 1.4
1:18	scaled	-132.9 ± 12.3	-138.8 ± 12.1	5.9 ± 1.1
1:10	original	-201.5 ± 26.8	-208.6 ± 26.8	7.1 ± 2.0
1:10	scaled	-128.9 ± 17.2	-137.0 ± 15.3	8.1 ± 4.1

References

(1) Akin-Ojo, O.; Song, Y.; Wang, F. Developing ab initio quality force fields from condensed phase quantum-mechanics/molecular-mechanics calculations through the adaptive force matching method. *J. Chem. Phys.* **2008**, *129*.

(2) Kühne, T. D.; Iannuzzi, M.; Del Ben, M.; Rybkin, V. V.; Seewald, P.; Stein, F.; Laino, T.; Khaliullin, R. Z.; Schütt, O.; Schiffmann, F.; others CP2K: An electronic structure and molecular dynamics software package-Quickstep: Efficient and accurate electronic structure calculations. *J. Chem. Phys.* **2020**, *152*.

(3) Jorgensen, W. L.; Maxwell, D. S.; Tirado-Rives, J. Development and testing of the OPLS all-atom force field on conformational energetics and properties of organic liquids. *J. Am. Chem. Soc.* **1996**, *118*, 11225–11236.

(4) Doherty, B.; Zhong, X.; Gathiaka, S.; Li, B.; Acevedo, O. Revisiting OPLS force field parameters for ionic liquid simulations. *J. Chem. Theory Comput.* **2017**, *13*, 6131–6145.

(5) Aqvist, J. Ion-water interaction potentials derived from free energy perturbation simulations. *J. Phys. Chem.* **1990**, *94*, 8021–8024.

(6) Ewald, P. P. Die Berechnung optischer und elektrostatischer Gitterpotentiale. *Ann. Phys. (Leipzig)* **1921**, *369*, 253–287.

(7) Essmann, U.; Perera, L.; Berkowitz, M. L.; Darden, T.; Lee, H.; Pedersen, L. G. A smooth particle mesh Ewald method. *J. Chem. Phys.* **1995**, *103*, 8577–8593.

(8) Perdew, J. P.; Burke, K.; Ernzerhof, M. Generalized gradient approximation made simple. *Phys. Rev. Lett.* **1996**, *77*, 3865.

(9) Grimme, S.; Antony, J.; Ehrlich, S.; Krieg, H. A consistent and accurate ab initio parametrization of density functional dispersion correction (DFT-D) for the 94 elements H-Pu. *J. Chem. Phys.* **2010**, *132*.

(10) Tang, W.; Sanville, E.; Henkelman, G. A grid-based Bader analysis algorithm without lattice bias. *J. Phys. Condens. Matter* **2009**, *21*, 084204.

(11) Sanville, E.; Kenny, S. D.; Smith, R.; Henkelman, G. Improved grid-based algorithm for Bader charge allocation. *J. Comput. Chem.* **2007**, *28*, 899–908.

(12) Henkelman, G.; Arnaldsson, A.; Jónsson, H. A fast and robust algorithm for Bader decomposition of charge density. *Comput. Mater. Sci.* **2006**, *36*, 354–360.

(13) Nelder, J. A.; Mead, R. A simplex method for function minimization. *Comput. J.* **1965**, *7*, 308–313.

(14) Virtanen, P. et al. SciPy 1.0: Fundamental Algorithms for Scientific Computing in Python. *Nat. Methods* **2020**, *17*, 261–272.

(15) Eastman, P.; Swails, J.; Chodera, J. D.; McGibbon, R. T.; Zhao, Y.; Beauchamp, K. A.; Wang, L.-P.; Simmonett, A. C.; Harrigan, M. P.; Stern, C. D.; others OpenMM 7: Rapid development of high performance algorithms for molecular dynamics. *PLoS Comput. Biol.* **2017**, *13*, e1005659.

(16) Jo, S.; Kim, T.; Iyer, V. G.; Im, W. CHARMM-GUI: a web-based graphical user interface for CHARMM. *J. Comput. Chem.* **2008**, *29*, 1859–1865.

(17) Brooks, B. R.; Brooks III, C. L.; Mackerell Jr, A. D.; Nilsson, L.; Petrella, R. J.; Roux, B.; Won, Y.; Archontis, G.; Bartels, C.; Boresch, S.; others CHARMM: the biomolecular simulation program. *J. Comput. Chem.* **2009**, *30*, 1545–1614.

(18) Lee, J.; Cheng, X.; Jo, S.; MacKerell, A. D.; Klauda, J. B.; Im, W. CHARMM-GUI input generator for NAMD, GROMACS, AMBER, OpenMM, and CHARMM/OpenMM simulations using the CHARMM36 additive force field. *Biophys. J.* **2016**, *110*, 641a.

(19) Choi, Y. K.; Park, S.-J.; Park, S.; Kim, S.; Kern, N. R.; Lee, J.; Im, W. CHARMM-GUI

polymer builder for modeling and simulation of synthetic polymers. *J. Chem. Theory Comput.* **2021**, *17*, 2431–2443.

(20) Thompson, A. P.; Aktulga, H. M.; Berger, R.; Bolintineanu, D. S.; Brown, W. M.; Crozier, P. S.; In't Veld, P. J.; Kohlmeyer, A.; Moore, S. G.; Nguyen, T. D.; others LAMMPS-a flexible simulation tool for particle-based materials modeling at the atomic, meso, and continuum scales. *Comput. Phys. Commun.* **2022**, *271*, 108171.

(21) Humphrey, W.; Dalke, A.; Schulten, K. VMD: visual molecular dynamics. *J. Mol. Graph.* **1996**, *14*, 33–38.